ELSEVIER

Journal of Molecular Catalysis A: Chemical 162 (2000) 307–316

JOURNAL OF MOLECULAR CATALYSIS A: CHEMICAL

www.elsevier.com/locate/molcata

Activities of supported copper oxide catalysts in the NO + CO reaction at low temperatures

Yuhai Hu, Lin Dong *, Jun Wang, Weiping Ding, Yi Chen

Institute of Mesoscopic Solid State Chemistry, Department of Chemistry, Nanjing University, Nanjing 210093, People's Republic of China

Abstract

The activities of copper oxide supported on CeO_2, γ-Al_2O_3 and ceria-modified γ-Al_2O_3 catalysts for the NO + CO reaction at low temperature (200°C) have been investigated. The results show that the activities of the surface-dispersed copper species are greatly enhanced due to the presence of ceria, whether it was used as a support or as the pre-dispersed species on γ-Al_2O_3. The activities decrease in the order: $CuO/CeO_2 > CuO/CeO_2/\gamma$-$Al_2O_3 > CuO/\gamma$-$Al_2O_3$. For the $CuO/CeO_2/\gamma$-Al_2O_3 catalysts, it is shown that NO conversions are not improved significantly with the increasing of CuO and/or ceria loadings, however, the turn-over number for the catalysts is found to be strongly relative to ceria loadings. By a combination of X-ray diffraction (XRD), electron spin resonance (ESR) and temperature programmed reduction (TPR) results, the states and properties of copper oxide species, as well as the interactions among the surface-dispersed copper oxide species, ceria species and support, are also studied. All the results are tentatively discussed according to the incorporation model proposed previously. © 2000 Published by Elsevier Science B.V.

Keywords: NO reduction; Supported catalysts; Ceria; CuO; ESR; XRD; TPR

1. Introduction

In the recent years, the reductive elimination of NO has been extensively studied for the purpose of controlling the exhaust emission, and most of the investigations have been focused on supported noble metal catalysts for the reduction of NO in the presence of CO [1–4]. However, the employment of noble metal catalysts is limited due to their scarce and high cost, and the substitution by the cheap metals for the noble metals has attracted much interests recently [5–7]. The catalysts containing transition metals, especially copper, show a potential activity in this reaction and have been extensively investigated during the past decades [8–10].

Generally, three forms of the copper containing catalysts have been used for the investigations, e.g. unsupported copper oxide catalysts [11], supported copper oxide catalysts and supported metal copper catalysts [12,13]. Meanwhile, the promotion of the doped ceria in the catalysts is of great studies in the studies for the supported copper oxide catalysts, because it is believed that doped ceria inhibits the deactivation of active components in the reaction due to the sintering of the metals and surface deterioration of the support [14,15]. Another aspect of ceria that has received the most intensive attention in the recent literatures is its role as an "oxygen storage" compound influencing the activities of the three-way catalysts in different reactions. Fernandez-Garcia et

* Corresponding author.
E-mail address: chem718@netra.nju.edu.cn (L. Dong).

1381-1169/00/$ - see front matter © 2000 Published by Elsevier Science B.V.
PII: S1381-1169(00)00299-5

al. [16] and Javier et al. [17] have carried out a series of works on the "oxygen storage" capacity of ceria and its influence on the dispersion and reduction/oxidation behaviors of alumina-supported copper catalysts. They pointed out that the copper–cerium interaction affected the reactivity of the catalysts towards NO, increasing the amount of adsorbed species, which led to low temperature NO and N_2/N_2O desorption, as well as shifting the decomposition temperatures of surface containing N–N bonds (N_2/N_2O) formed upon NO adsorption. Li and Yang [18], in their studies about the selective adsorption of NO_x from hot combustion gases by Ce-doped CuO/TiO_2 pointed out that 5% CuO/TiO_2 showed to be a superior sorbent for selective, reversible adsorption of NO from hot combustion gases, and doping with 2% Ce on the CuO/TiO_2 sorbent further increased both uptake (50% increase in initial rate) and the NO_x capacity (by 30%). Studies on the states of the doped ceria species in the catalysts were also carried out in Shyu's laboratory by using X-ray photoelectron spectroscopy (XPS), Raman spectroscopy and temperature programmed reduction (TPR), and three cerium species were detected, namely, a $CeAlO_3$ precursor in the dispersed phase, small CeO_2 particles and large CeO_2 particles [19].

Despite of the extensive studies mentioned above, the role of the doped ceria and the nature of the interactions among the ceria and the active species, as well as the support, are still open to study. In the present work, the catalytic activities of the CuO/CeO_2, $CuO/\gamma\text{-}Al_2O_3$ and $CuO/CeO_2/\gamma\text{-}Al_2O_3$ catalysts with different CuO and ceria loadings in the NO + CO reaction at 200°C were investigated. The results showed that the activities of the catalysts are strongly related to ceria species, either as a support or as a surface-dispersed species. In addition, the results were tentatively discussed by using the incorporation model proposed previously [20].

2. Experimental

2.1. Instruments

XRD (X-ray diffraction) patterns were obtained with a Shimadzu XD-3A diffractomer employing Ni-Kα radiation (0.15418 nm), the X-ray tube was operated at 35 kV and 20 mA.

Brunauer–Emmet–Teller (BET) surface areas were measured by nitrogen adsorption at 77 K on a Micrometrics ASAP-2000 adsorption apparatus.

Electron spin resonance (ESR) spectra were recorded on a FE1XG Electron Spinning Resonance Spectrometer at liquid nitrogen temperatures. The catalysts were put into a glass tube, and then calcined at 300°C for 3 h to remove the adsorbed impurities before sealed.

TPR was carried out in a quartz U-tube reactor, and a 30-mg catalyst was used for each measurement. Prior to the reduction, the catalyst was pretreated in a N_2 stream at 100°C for 1 h and then cooled to room temperature. After that, a H_2–N_2 mixture (5% by volume) was switched on. The temperature was increased linearly at a rate of 10 K min^{-1}.

2.2. Catalyst preparation

$\gamma\text{-}Al_2O_3$, obtained from Fusun Petrochemical Institute in China, was calcined at 700°C for 5 h before using for preparing supported catalysts; the BET surface area was 195 $m^2\ g^{-1}$.

CeO_2 was obtained by thermal decomposition of $Ce(NO_3)_3 \cdot 6H_2O$ in air at 550°C for 5 h; the BET surface area was 58 $m^2\ g^{-1}$.

Ceria-modified $\gamma\text{-}Al_2O_3$ supports were prepared by incipient wetness impregnation of $\gamma\text{-}Al_2O_3$ with an aqueous solution containing the requisite amount of $Ce(NO_3)_3$. The catalysts were dried in air at 100°C for 24 h and then calcined at 450°C for 3.5 h.

CuO-supported catalysts with different CuO loadings were prepared by incipient wetness impregnation of CeO_2, $\gamma\text{-}Al_2O_3$ or $CeO_2/\gamma\text{-}Al_2O_3$ supports with an aqueous solution containing the requisite amount of copper nitrate hexahydrate, respectively. The catalysts were dried at 100°C for 24 h, and then calcined at 450°C in air for 3.5 h. A list of these catalysts with the different CuO or ceria loadings is given in Table 1. In this table and in the rest of this paper, both commonly used units for CuO or ceria loadings were employed, namely, weight percent (wt.%) and millimoles of CuO or CeO_2 per 100 m^2 of surface area of CeO_2 or $\gamma\text{-}Al_2O_3$. Meanwhile, for the sake of convenience, catalysts CuO/CeO_2,

Table 1
CuO and ceria loadings in different catalysts

Catalysts	CuO loading		Ceria loading	
	mmol/100 m^2 γ-Al_2O_3	wt.%	mmol/100 m^2 γ-Al_2O_3	wt.%
CuAl	0.1	1.53		
	0.4	5.86		
	0.8	11.1[a]		
	1.2	15.8		
	1.8	21.9		
	2.4	27.2		
CuCe	0.1	0.43		
	0.3	1.27		
	0.6	2.50		
	1.2	4.89[a]		
	1.8	7.15		
	2.4	9.32		
CuCeAl	0.8	10.56	0.15	4.26
	0.8	10.01	0.30	8.21
	0.8	8.11	1.20	25.4
CuCeAl	0.4	5.56	0.15	4.49
	0.4	5.31	0.30	8.61
	0.4	4.23	1.20	27.5

[a]Catalysts with the copper oxide loadings at about the dispersion capacities on the supports.

CuO/γ-Al_2O_3 and $CuO/CeO_2/\gamma$-Al_2O_3 will be hereafter signed as CuCe, CuAl and CuCeAl, respectively.

The activities of the catalysts were determined under steady state, involving a feed steam with a fixed composition, NO 5%, CO 10% and He 85% by volume as a dilutent. A quartz U-tube with a requisite quantity of catalyst ($\sim$100 mg) was used. The catalysts were pretreated in He stream at 100°C for 1 h and then cooled to room temperature, after that, the mixed gases were switched on. The reactions were carried out at different temperatures with a space velocity of 5000 h^{-1}. Two volumes and thermal conduction detections (TCDs) were used for the purpose of analyzing the production, volume A with Paropak P for separating N_2O and CO_2, and volume B, packed with 5A zeolite (40–60 M) for separating N_2, NO and CO.

3. Results

3.1. XRD results

XRD results of CuCe catalysts with different CuO loadings are shown in Fig. 1. Peaks corresponding to the crystalline CuO did not appear in the catalysts with CuO loadings of $\leq$1.2 mmol/100 m^2 CeO_2, which indicated that all the copper oxide species were highly dispersed on the surface of CeO_2. As the CuO loadings were beyond 1.2 mmol/100 m^2 CeO_2, two peaks corresponding to the crystalline CuO were observed ($2\theta = 35.44°$, 38.78°), as shown in Fig. 1(e) and (f). This result was consistent with our previous report that the dispersion capacity of CuO on the surface of CeO_2 was 1.2 mmol/100 m^2 CeO_2 [21]. For the catalysts with higher CuO loadings ($>$1.2 mmol/100 m^2 CeO_2), crystalline CuO was formed beside the surface-dispersed copper oxide species.

XRD patterns of CuAl catalysts with different CuO loadings are shown in Fig. 2. For catalysts with CuO loadings lower than 0.8 mmol/100 m^2 γ-Al_2O_3, evident peaks corresponding to the crystalline CuO were not observed, as shown in Fig. 2(a) and (b), which implied that the copper oxide species was highly dispersed on the surface of γ-Al_2O_3. When the CuO loadings were increased, crystalline CuO appeared of increasing intensity with CuO loadings, which indicated that crystalline CuO has been formed. As discussed in our previous work, Cu^{2+}

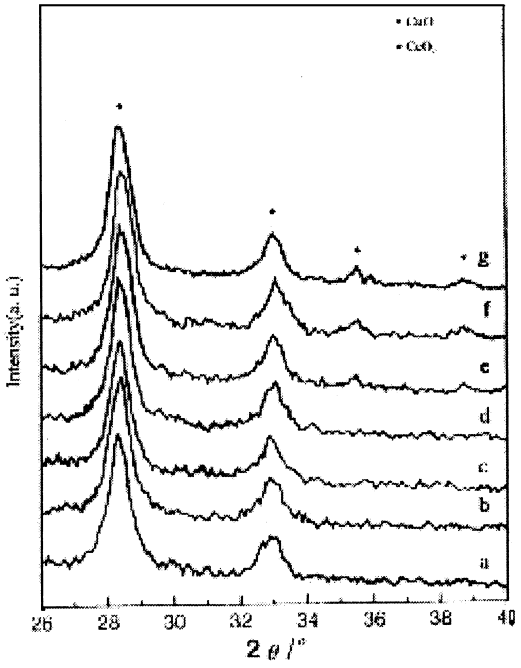

Fig. 1. XRD patterns: (a), (b), (c), (d), (e) and (f), for CuCe catalysts with CuO loadings 0.1, 0.3, 0.6, 1.2, 1.8 and 2.4 mmol/100 m^2 CeO_2 respectively; (g) mixture of CuO (1.8 mmol/100 m^2 CeO_2) with crystalline CeO_2.

ions in the CuAl catalysts have a preference to incorporate into the octahedral vacant sites in the surface lattice of γ-Al_2O_3 when calcined at 450°C, leading to the dispersion capacity is only about half of the value expected for all the MO/γ-Al_2O_3 catalysts (about 1.50 mmol/100 m^2 γ-Al_2O_3) [20,22], in which MO represents NiO, ZnO, CdO and MgO, etc.

XRD results of CeAl catalysts with different ceria loadings are shown in Fig. 3. Peaks corresponding to crystalline CeO_2 were not detected for the catalyst of 0.15 mmol/100 m^2 γ-Al_2O_3, indicating that cerium oxide species was highly dispersed on the surface of γ-Al_2O_3. Typical diffraction lines of crystalline CeO_2 were present in the XRD patterns for the catalysts with higher ceria loadings ($\geq$ 0.3 mmol/100 m^2 γ-Al_2O_3), as shown in pattern in Fig. 3(b). It seemed to suggest that the crystalline CeO_2 have also been formed in these catalysts beside the surface-dispersed cerium oxide species. This result was in agreement with the recent report by Shyu et al. [19], in which the surface-dispersed and the small CeO_2 particles had been found for the sample with a ceria

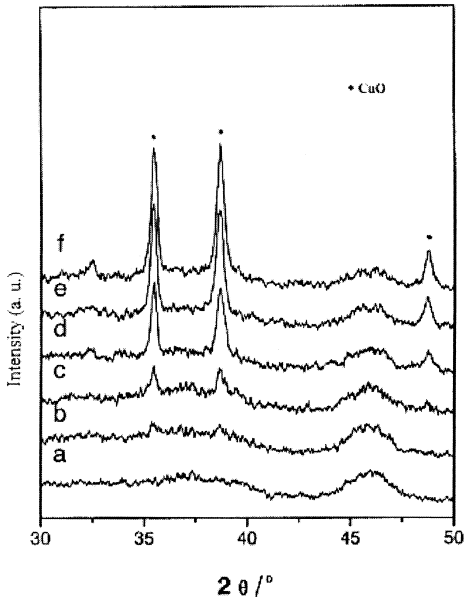

Fig. 2. XRD patterns: (a), (b), (c), (d), (e) and (f), for CuAl catalysts with CuO loadings 0.1, 0.4, 0.8, 1.2, 1.8 and 2.4 mmol/100 m^2 γ-Al_2O_3, respectively.

loading of 0.27 mmol/100 m^2 γ-Al_2O_3, implying that the dispersion capacity of ceria on γ-Al_2O_3 was lower than 0.27 mmol/100 m^2 γ-Al_2O_3.

XRD patterns of CuCeAl catalysts containing different ceria and CuO loadings are shown in Fig. 4. The result shows that the XRD patterns became

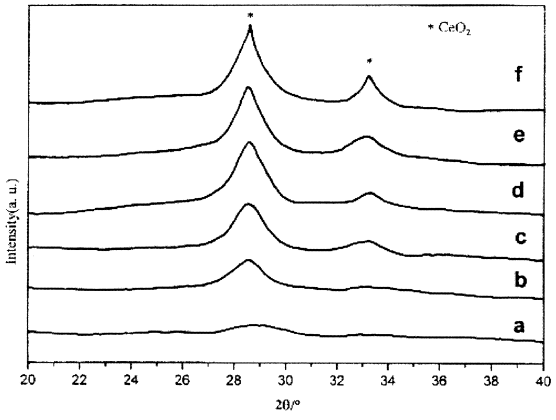

Fig. 3. XRD patterns: (a), (b), (c), (d), (e) and (f), for CeAl catalysts with ceria loadings 0.15, 0.3, 0.6, 1.2, 1.8 and 2.4 mmol/100 m^2 γ-Al_2O_3, respectively.

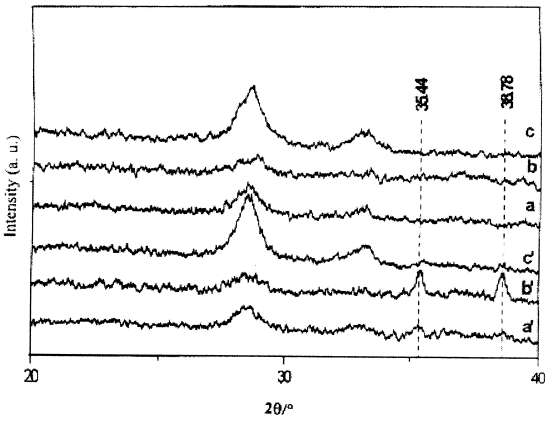

Fig. 4. XRD patterns: (a), (b) and (c), for CuCeAl catalysts with a fixed CuO loading of 0.4 mmol/100 m^2 γ-Al_2O_3 and various ceria loadings of 0.15, 0.3 and 1.2 mmol/100 m^2 γ-Al_2O_3, respectively; (a′), (b′) and (c′), for CuCeAl catalysts with a fixed CuO loading of 0.8 mmol/100 m^2 γ-Al_2O_3 and various ceria loadings 0.15, 0.3 and 1.2 mmol/100 m^2 γ-Al_2O_3, respectively.

complex as compared to the CeAl catalysts. For the CuCeAl catalysts with a fixed CuO loading of 0.4 mmol/100 m^2 γ-Al_2O_3 and varying ceria loadings, peaks of crystalline CuO were not observed, indicating that copper oxide species was highly dispersed on the surface of the supports, e.g. γ-Al_2O_3 and/or CeO_2. For the CuCeAl catalysts with a fixed CuO loading of 0.8 mmol/100 m^2 γ-Al_2O_3 and lower ceria loadings ($\leq$0.3 mmol/100 m^2 γ-Al_2O_3), diffraction lines identified as crystalline CuO were observed, and the more ceria was loaded, the stronger was peak intensity of the crystalline CuO present in the catalysts, as seen by comparing Fig. 4(a′) and (b′). However, when ceria loading was increased to 1.2 mmol/100 m^2 γ-Al_2O_3, the peaks corresponding to crystalline CuO disappeared, as shown in Fig. 4(c′). It seemed that for the two CuCeAl catalysts with ceria loadings $\leq$0.3 mmol/100 m^2 γ-Al_2O_3, crystalline CuO existed beside the surface-dispersed copper oxide species. For the catalyst with a ceria loading of 1.2 mmol/100 m^2 γ-Al_2O_3, the disappearance of the crystalline CuO could be attributed to the dispersion of copper oxide on the surface of CeO_2 particles. This result suggested that, for the CuCeAl catalyst with the ceria loading beyond its dispersion capacity, it could be regarded as mixtures of CuO/CeO_2/γ-Al_2O_3 and CuO/CeO_2.

3.2. ESR results

ESR results of the dispersed copper oxide species for CuCe and CuAl catalysts are shown in Fig. 5, the six asymmetric signals are ascribed to the manganese reference (e.g. $g = 2.0329$), and the two catalysts presented some evident differences. The ESR spectroscopy of CuAl catalyst presented an asymmetric, narrow signal displaying extremum at about 2.06, while the ESR spectroscopy of CuCe catalyst showed an asymmetric, obviously broadened and unresolved signal. Its intensity was also weaker than that of CuAl catalyst. It seemed to suggest that the difference of the spectra could be attributed to the different coordination environments of the Cu^{2+} ions in the surface-dispersed copper species [16]. Otherwise, The ESR spectroscopy of the surface-dispersed copper oxide species (0.4 mmol/100 m^2 γ-Al_2O_3) on the mixed support, γ-Al_2O_3 and CeO_2, (20 wt.%, CeO_2), presented an asymmetric and slightly broader signal than the CuAl catalyst with the same CuO loading, by comparing the signal of Fig. 5(b) and (c). This might be due to an over-lapping of the signals of the copper oxide species dispersed on the surface of the γ-Al_2O_3 and CeO_2 supports.

ESR results of the CuCeAl catalysts also presented an asymmetric, narrow signal displaying extremum at 2.06, which was similar to that of CuAl. But there was another weak peak centered at 2.23, as shown in Fig. 6(a) and (b), and it was only detected in the CuCeAl catalysts containing small CuO crys-

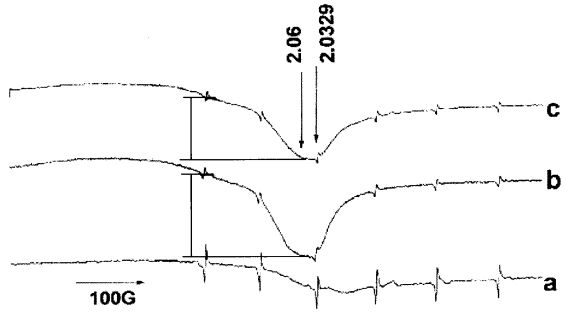

Fig. 5. ESR results of various CuO-supported catalysts: (a) CuCe catalysts with CuO loading 0.3 mmol/100 m^2 CeO_2; (b) CuAl catalysts with CuO loading of 0.4 mmol/100 m^2 γ-Al_2O_3; (c) CuO (0.4 mmol/100 m^2 γ-Al_2O_3) supported on mixed γ-Al_2O_3 and CeO_2 (20 wt.%, CeO_2).

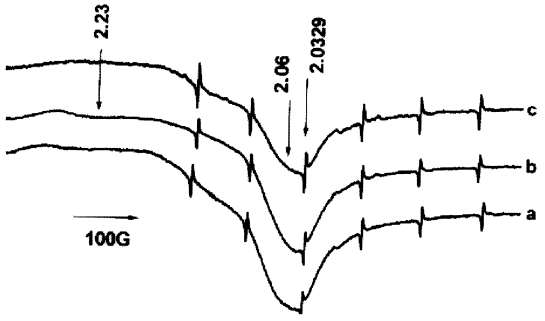

Fig. 6. ESR results of CuCeAl catalysts with a fixed CuO loading of 0.8 mmol/100 m^2 γ-Al_2O_3 and various ceria loadings: (a) 0.15, (b) 0.3, and (c) 1.2 mmol/100 m^2 γ-Al_2O_3, respectively.

tallites. This signal vanished for the catalyst with a ceria loading above 1.2 mmol/100 m^2 γ-Al_2O_3, in which the crystalline CuO has been found to disappear in the XRD result. It has been assumed that this signal corresponded to the Cu^{2+} cluster in the copper oxide supported catalysts [23]. Furthermore, the ESR spectroscopy of the CuCeAl catalyst with a ceria loading of 1.2 mmol/100 m^2 γ-Al_2O_3 also presented a broader signal than the CuCeAl catalysts with ceria loadings of ≤ 0.3 mmol/100 m^2 γ-Al_2O_3, which was more or less similar to the surface-dispersed copper oxide on the mixed support, γ-Al_2O_3 and CeO_2. It seemed to suggest that the disappearance of crystalline CuO should be resulted from a further dispersion of CuO on the surface of formed CeO_2 particles in CuCeAl catalysts with high ceria loadings.

3.3. Activity results

Fig. 7 shows the activities of the three kinds of catalysts in the NO + CO reaction at 200°C. At this reactant temperature, products were not detected in the tail gas for crystalline CuO, crystalline CeO_2 or CeO_2/γ-Al_2O_3 catalysts, which were not active in the reactant conditions. For the CuAl catalysts, the NO conversion increased with the CuO loadings initially, and reached a maximum when the CuO loadings reached its dispersion capacity, then decreased with increasing CuO loadings, as shown in Fig. 7(a). Unlike the CuAl catalysts, the NO conversions kept increasing slightly for the CuCe catalysts with CuO loadings beyond the dispersion capacity, as shown in Fig. 7(d). According to the XRD results, it seemed to suggest that the active component for the CuO-supported catalysts under this condition was the surface-dispersed copper oxide species. The decrease of the NO conversions for the CuAl catalysts with higher CuO loadings might be due to: (1) part of the surface-dispersed copper oxide species covered by the formed crystalline CuO, and (2) the decrease of the surface copper oxide species relative to the total copper oxide in the catalysts, as a consequence of the formation of the bulk CuO. The result that NO conversions still kept increasing slightly as CuO loadings were beyond the dispersion capacity, as shown for the CuCe catalysts, might be due to the moderate reduction of the surface-dispersed copper oxide species. For CuCeAl catalysts, NO conversions did not change greatly as the CuO loadings increased from 0.4 to 0.8 mmol/100 m^2 γ-Al_2O_3, or ceria loadings vary from 0.15 to 1.2 mmol/100 m^2 γ-Al_2O_3, shown as in Fig. 7(b) and (c). Furthermore, it was worth noting that the NO conversions

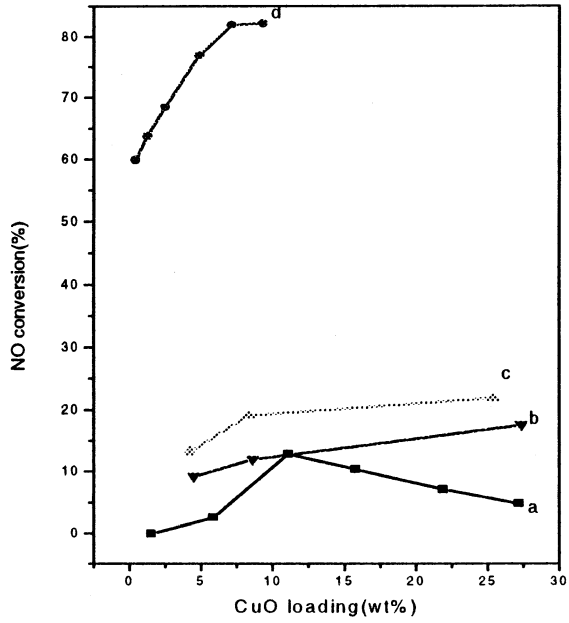

Fig. 7. Comparison of NO conversions over different CuO-supported catalysts with space velocity of 5000 h^{-1} at 200°C: (a) CuAl catalysts; (b) CuCeAl catalysts with a fixed CuO loading 0.4 mmol/100 m^2 γ-Al_2O_3; (c) CuCeAl catalysts with a fixed CuO loading of 0.8 mmol/100 m^2 γ-Al_2O_3; and (d) CuCe catalysts.

over CuCeAl catalysts were higher than that over CuAl catalysts by comparison of (b) and (c) to (a).

Some interesting results will also be obtained by comparing the turn-over number of the catalysts, CuCe, CuAl and CuCeAl. The turn-over number for the CuCe and CuAl catalysts were obtained by normalizing the NO conversions to the total amount of the surface-dispersed copper oxide species. The turn-over number for the CuCeAl catalysts was obtained by normalizing the NO conversions to the total amount of copper oxide species in the catalysts (including the surface-dispersed copper oxide species on γ-Al_2O_3 and/or CeO_2, and the formed crystalline CuO). As shown in Table 2, the turn-over number for CuCe catalyst were one or two orders of magnitude higher than that for the CuAl catalysts. These results suggested that the catalytic activity of the dispersed copper oxide species in CuCe catalysts have been greatly enhanced, as compared to that in CuAl catalysts. For the CuCeAl catalysts with low ceria loading, higher CuO loadings led to a decrease of the turn-over number, which supported the former proposal that the surface-dispersed copper oxide species in the catalysts were the active components under this condition. However, the turn-over number was increased with ceria loadings, especially for the catalysts with 1.2 mmol/100 m^2 γ-Al_2O_3 loaded, which showed an activity even at 100°C. Recall the activity for the CuCe catalysts, which also showed a reactivity towards NO reduction at 100°C, the activity for the CuCeAl catalysts at 100°C could be probably ascribed to the dispersed copper oxide species on crystalline CeO_2. The results suggested that doped cerium oxides, especially crystalline CeO_2 as a support, exhibited high ability to promote surface-dispersed copper oxide species towards NO + CO reaction, and the activities increased in the order: CuAl < CuCeAl < CuCe.

4. Discussion

4.1. The possible structures of ceria on γ-Al_2O_3, and copper oxide on ceria-modified γ-Al_2O_3

As reported by Shyu et al. [19], the surface-dispersed ceria species was similar to $CeAlO_3$ formed by the strong interactions between CeO_2 and γ-Al_2O_3, but the nature of the interaction has not been discussed there. Based on the incorporation model, structure of incorporated Ce^{4+} ions in the C-layer of γ-Al_2O_3 was taken as an example for discussion as

Table 2
The turn-over number of different catalysts at different temperatures

Catalyst	CuO loading (mmol/100 m^2 γ-Al_2O_3)	Ceria loading (mmol/100 m^2 γ-Al_2O_3)	Turn-over number	
			100°C	200°C
	0.1		65	1044
	0.3		54	374
	0.6		47	207
CuCe	1.2		34	117
	1.8		24	121
	2.4		21	129
	0.1		0	0
	0.4		0	3
	0.8		0	9
CuA1	1.2		0	8
	1.8		1	3
	2.4		0	1
	0.4	0.15	0	27
CuCeA1	0.4	0.3	0	37
	0.4	1.2	15	68
	0.8	0.15	0	20
CuCeA1	0.8	0.3	0	31
	0.8	1.2	5	44

shown in Fig. 8. Due to the strong interaction with the support, the surface-dispersed ceria species will present different properties as compared to the crystalline CeO_2, as was revealed by the TPR (H_2) results in Gandhi's studies. As has been shown, the surface-dispersed ceria species was more easily reduced to $CeAlO_3$ than the particle CeO_2 on γ-Al_2O_3, and the reduction temperature was lower than the crystalline CeO_2 [19]. Furthermore, they also reported that the saturation loading for ceria on the surface of γ-Al_2O_3 was only 0.28 mmol/100 m^2 γ-Al_2O_3, which was less than that for the MO_2/γ-Al_2O_3 systems, such as TiO_2 or ZrO_2 (0.56 mmol/100 m^2 γ-Al_2O_3) [24,25]. It was assumed that part of the surface vacant sites of γ-Al_2O_3 could not be occupied when ceria was dispersed. The above postulation was partially supported by our previous considerations on the γ-Al_2O_3-supported KCl and NaCl catalysts, for which the dispersion capacity of KCl on γ-Al_2O_3 was reported to be about 0.35 mmol/100 m^2 γ-Al_2O_3 lower than NaCl [26], probably due to the large radius of K^+.

For CuCeAl catalysts, the Ce^{4+} ions would occupy some of the surface octahedral vacant sites of γ-Al_2O_3 at the pre-impregnation procedure, and the Cu^{2+} ions would incorporate into the residual surface octahedral sites. At the same time, the dispersed copper oxide species could share the capping O^{2-} ions offered by the nearby dispersed ceria to form an octahedral surface copper species, as shown in Fig. 8. When ceria loadings were beyond the dispersion capacity of CeO_2 on γ-Al_2O_3, the CeAl catalysts could be regarded as the mixture of the CeO_2-modified γ-Al_2O_3 and CeO_2 supports. In this case, Cu^{2+} ions could disperse on the unoccupied octahedral vacancies of the CeO_2-modified γ-Al_2O_3 and on the formed crystalline CeO_2, simultaneously.

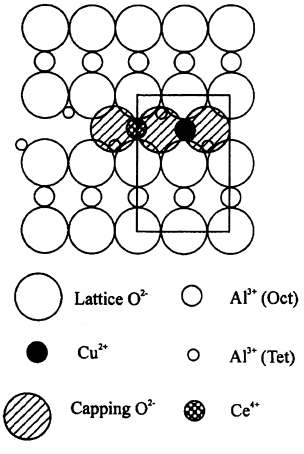

Fig. 8. The schematic diagram for the incorporated Ce^{4+} ions and its neighboring Cu^{2+} ions in the surface vacant site of the (110) plane of γ-Al_2O_3.

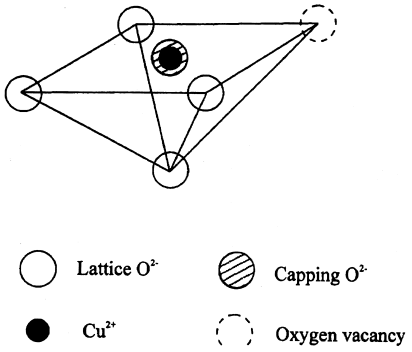

Fig. 9. The schematic diagram for the incorporated Cu^{2+} ions in the surface vacant site of the (110) plane of γ-Al_2O_3.

For dispersed copper oxide species in the CuAl catalysts calcined at 450°C, a defect octahedral structure is formed (actually, five-coordinated with O^{2-} ions) due to Cu^{2+} ions incorporated into the octahedral vacant sites of γ-Al_2O_3, as shown in Fig. 9. The dispersed CuO on CeO_2 also forms a five-coordinated copper oxide species with Cu^{2+} ions incorporating into the cubic vacant sites on the preferentially exposed plane (111) of CeO_2, as shown in Fig. 10. Even if the five-coordinated surface copper oxide

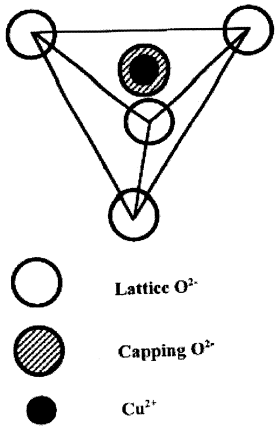

Fig. 10. The schematic diagram for the incorporated Cu^{2+} ions in the surface vacant site of the (111) plane of CeO_2.

species were formed both on CeO_2 and γ-Al_2O_3, different Cu–O bonds of the surface-dispersed copper oxide species, induced by different surface structures of the supports, resulted in the different properties of the dispersed copper oxide species.

TPR profiles for the crystalline CuO, CuAl and CuCe catalysts with CuO loadings below its dispersion capacity were shown in Fig. 11. Reduction of crystalline CuO was observed when the temperature was increased higher than 290°C, and only one peak could be observed as shown in curve *a*. Two peaks were detected at approximately 190°C and 239°C for the CuCe catalyst. The TPR profile could be interpreted as a stepwise reduction of the surface-dispersed CuO. The peak at 190°C was probably associated with the reduction from Cu^{2+} to Cu^{1+}, and the other at 239°C was likely due to the reduction from Cu^{1+} to Cu^0 [21]. While for CuAl catalyst, only one peak at 252°C was observed, this reduction temperature was higher than that associated with the reduction of dispersed copper species on CeO_2, but lower than that of crystalline CuO. The lower reduction temperatures for the supported copper oxide species than that of crystalline CuO, as well as the lower temperature for CuO-supported on CeO_2 than on γ-Al_2O_3, should be presumably attributed to the influence of the supports.

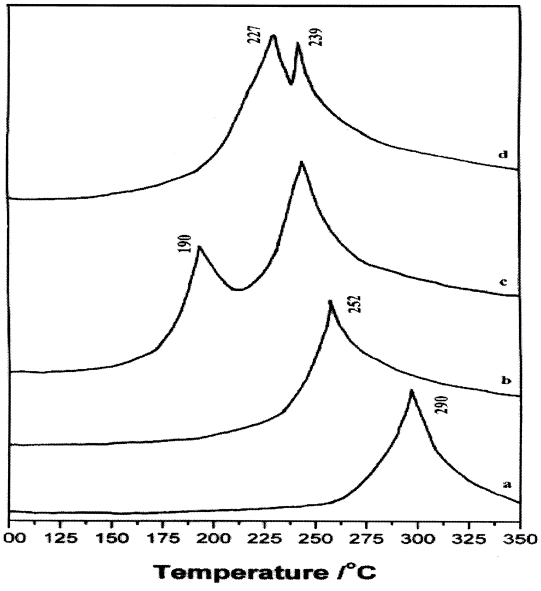

Fig. 11. TPR profiles of various catalysts: (a) crystalline CuO; (b) CuAl catalysts with a CuO loading of 0.4 mmol/100 m^2 γ-Al_2O_3; (c) CuCe catalysts with a CuO loading of 0.3 mmol/100 m^2 CeO_2; (d) CuCeAl catalysts with a fixed CuO loading of 0.8 mmol/100 m^2 γ-Al_2O_3 and ceria loading of 0.15 mmol/100 m^2 γ-Al_2O_3, respectively.

As shown in Fig. 11(d), the TPR profile showed two peaks at 227°C and 239°C for the CuCeAl catalyst (with CuO loading 0.8 mmol/100 m^2 γ-Al_2O_3 and ceria loading 0.15 mmol/100 m^2 γ-Al_2O_3), which were lower than that associated with the reduction of CuO supported on γ-Al_2O_3. The peak at 227°C was probably associated with reduction of the surface-dispersed copper oxide species, and the other one at 239°C was likely due to the reduction of the small CuO crystallite. This result meant that copper oxide species dispersed on γ-Al_2O_3 is easier to be reduced when CeO_2 was doped. Considering the structure of copper oxide species shown in Fig. 8, the dispersed copper oxide species has direct interactions with γ-Al_2O_3 and the dispersed ceria on γ-Al_2O_3, simultaneously, and the properties of the dispersed copper oxide species should be different from those shown in CeO_2 or γ-Al_2O_3 supported copper oxide, respectively.

4.2. Surface reactivity towards NO reduction

As proposed by Shelef and Kummers [27], the reduction of NO in the presence of CO could proceed in two steps: first, a partial reduction from NO to N_2O; and second, a subsequent reduction from N_2O to N_2. Each of the steps corresponded to the oxidation of a reduced site, and therefore, the majority of oxygen obtained by NO is liberated, accompanied by the formation of a more positive site. Along these lines, the prerequisite to the reduction of NO in the presence of CO on CuO and CuO-supported catalysts was a coordinatively unsaturated Cu^{2+} site for the adsorption of NO molecules, and a reduced copper site to receive the O^{2-} ions produced by NO decomposition. It was relatively difficult to obtain a reduced copper site for CuO-supported γ-Al_2O_3 catalysts at 200°C according to the TPR results, which resulted in the lower activity for the CuAl catalysts in NO + CO reaction than CuCe catalysts. For the CuCeAl catalysts, because of the promotion of the surface-dispersed ceria and/or residual crystalline CeO_2, the surface-dispersed copper oxide species were more active for the reduction, and exhibited a

higher activity in the NO + CO reaction than CuAl catalysts.

5. Conclusions

(1) At 200°C, CeO_2- and γ-Al_2O_3-supported copper oxide catalysts showed a higher activity for the NO + CO reaction than crystalline CuO, and the ceria-supporting CuO catalyst exhibited a highest activity in the three kinds of catalysts. The results indicated that the different supports have different influence on the properties of surface-dispersed copper oxide species.

(2) The comparison of the activity results of CuAl and CuCeAl catalysts showed that the copper oxide species dispersed on the ceria-modified γ-Al_2O_3 were more active in the NO + CO reaction at 200°C, which was mainly due to the promotion of the doped ceria to dispersed copper oxide species, and/or the dispersed copper oxide species on the surface of the formed CeO_2 particles.

Acknowledgements

The financial support of the Special Foundation for the Doctor-subject of China (no. 98028434) is gratefully acknowledged.

References

[1] T.P. Kobylinski, B.W. Taylor, J. Catal. 33 (1974) 376.
[2] R.L. Klimish, K.C. Taylor, Environ. Sci. Technol. 7 (1993) 127.
[3] W.C. Hekker, A.T. Bell, J. Catal. 84 (1983) 220.
[4] S.H. Oh, C.C. Zickel, J. Catal. 128 (1990) 526.
[5] V.I. Parvulescu, P. Grange, B. Delmon, Catal. Today 46 (1998) 233.
[6] M. Iwamoto, H. Yahiro, Y. Torikai, T. Yoshioka, N. Mizuno, Chem. Lett. (1990) 1967.
[7] P. Oelker, V.I. Parvulescu, P. Grange, B. Delmon, Book of Abstract of IFEC '95, Tokyo, 1995.
[8] H. Wise, R.T. Rewick, J. Catal. 40 (1975) 301.
[9] F. Boccuzzi, E. Gulielminotti, G. Martra, G. Cerrato, J. Catal. 146 (1994) 449.
[10] M.C. Wu, D.W. Goodman, J. Phys. Chem. 98 (1994) 9874.
[11] J.W. London, A.T. Bell, J. Catal. 31 (1973) 96.
[12] C. Hierl, H.P. Urbach, H. Knozinger, J. Chem. Soc., Faraday Trans. 88 (1992) 355.
[13] A.R. Balkenede, H. den Daas, M. Huisman, O.L.J. Gijzeman, J.W. Geus, Appl. Surf. Sci. 47 (1991) 341.
[14] P.O. Larssen, A. Andersson, J. Catal. 179 (1998) 72.
[15] W. Liu, A.F. Sarofin, M. Flytzani-Stephanopoulos, Chem. Eng. Sci. 49 (1994) 4871.
[16] M. Fernandez-Garcia, E.G. Rebollo, A.G. Ruiz, J.C. Conesa, J. Soria, J. Catal. 172 (1997) 146.
[17] S. Javier, J.M. Coronado, J.C. Conesa, J. Chem. Soc., Faraday Trans. 92 (1996) 1619.
[18] W.B. Li, R.T. Yang, Energy Fuels 11 (1997) 428.
[19] J.Z. Shyu, W.H. Weber, H.S. Gandhi, J. Phys. Chem. 100 (1996) 845.
[20] Y. Chen, L.F. Zhang, Catal. Lett. 12 (1992) 51.
[21] L. Dong, Y.S. Jin, Y. Chen, Sci. China, Ser. B 40 (1997) 24.
[22] W.S. Xia, H.L. Wan, Y. Chen, J. Mol. Catal. 138 (1999) 185.
[23] R. Deen, P.I.T. Scheltus, G.D. Veies, J. Catal. 41 (1976) 218.
[24] W. Wei, L.Y. Duan, C.B. Wang, T.C. Xie, Nat. Gas Chem. Ind. 19 (1994) 20.
[25] W.A. Stranick, M. Houalla, D.M. Hercules, J. Catal. 106 (1987) 362.
[26] Y. Chen, L. Dong, Y.S. Jin, B. Xu, W.J. Ji, Stud. Surf. Sci. Catal. 101 (1996) 1293.
[27] M. Shelef, J.T. Kummers, Chem. Eng. Prog., Symp. Ser. 67 (1972) 115.